Laboratory studies of thermally processed H₂O-CH₃OH-CO₂ ice mixtures and their astrophysical implications

P. Ehrenfreund[1,2], **O. Kerkhof**[1,2], **W.A. Schutte**[2], **A.C.A. Boogert**[5], **P.A. Gerakines**[3,4], **E. Dartois**[5], **L. d'Hendecourt**[5], **A.G.G.M. Tielens**[6], **E.F. van Dishoeck**[1], and **D.C.B. Whittet**[3]

[1] Leiden Observatory, P.O. Box 9513, 2300 RA Leiden, The Netherlands
[2] Raymond and Beverly Sackler Laboratory for Astrophysics at Leiden Observatory, P.O. Box 9513, 2300 RA Leiden, The Netherlands
[3] Department of Physics, Applied Physics and Astronomy, Rensselaer Polytechnic Institute, Troy, NY 12180-3590, USA
[4] NASA/Goddard Space Flight Center, Mail Code 691, Greenbelt, MD 20771, USA
[5] Institute d'Astrophysique Spatiale, Campus d'Orsay, F-91405 Orsay, France
[6] Kapteyn Astronomical Institute, P.O. Box 800, 9700 AV Groningen, The Netherlands

Abstract. Data of the Infrared Space Observatory ISO have strongly influenced the current view of interstellar ice chemistry. ISO and ground-based results have confirmed that the most abundant ice species in warm regions close to massive protostars are H_2O, CO_2, and CH_3OH. Ice segregation in those environments reflects the extensive thermal processing of grains over the lifetime of protostars. We present here a systematic set of laboratory infrared spectra of ice mixtures dominated by H_2O, CO_2 and CH_3OH which have been exposed to thermal and UV irradiation processing. It is shown that the infrared bands of CO_2 and of CH_3OH are particularly sensitive to the ice composition, temperature and applied UV irradiation. The laboratory data suggest partial crystallization of interstellar ices in the protostellar environment. We present a detailed laboratory study of the CO_2 bending mode at 15.2 μm. The observed multipeak structure of the CO_2 bending mode is a result of thermal processing and can not be produced by UV irradiation in the laboratory. Laboratory results show that annealed CO_2 ice has a lower stability against UV irradiation than cold amorphous CO_2 ice. Annealed ice mixtures containing H_2O, CO_2 and CH_3OH show that the multipeak structure of the CO_2 bending mode is not destroyed by UV fluxes of $\lesssim 10^{18}$ photons·cm^{-2}. Detailed analysis of H_2O, CO_2 and CH_3OH bands show that their profiles can be effectively used to trace the line of sight conditions and the origin and evolution of the ice composition in dense clouds. The datafiles discussed in this paper can be retrieved from the Leiden observatory database (www.strw.leidenuniv.nl/∼lab/isodb).

Key words: methods: laboratory – ISM: abundances – ISM: dust, extinction – ISM: evolution – ISM: molecules – infrared: ISM: lines and bands

1. Introduction

Interstellar ices coat the dust grains inside cold dense clouds. Ground-based observations have revealed solid H_2O and CO as the most abundant ice species in the interstellar medium (ISM). Those species are observed toward numerous protostars as well as background sources (e.g. Chiar et al. 1998). Recent ground-based observations showed that CH_3OH and NH_3 are abundant in the line of sight toward some massive protostars (Dartois et al. 1999a, Lacy et al. 1998). The Infrared Space Observatory ISO has provided extraordinary results concerning the nature of dust particles (see special issue of A&A 315, 1996 and d'Hendecourt et al. 1999). During its operational phase ISO measured the complete mid-infrared spectrum (λ = 2.3–43 μm) of ices in many protostellar regions, free from telluric contamination. ISO led to new insights into the composition of interstellar ices, thermal processing in the protostellar vicinity and gas-grain chemistry (Whittet et al. 1996, d'Hendecourt et al. 1996, Ehrenfreund et al. 1998, Gerakines et al. 1999, Boogert et al. 1999a). Abundances of many ice species in bright star-forming regions have been derived from observations with the Short-Wavelength Spectrometer (SWS).

A major discovery of ISO was the ubiquitous presence of CO_2 ice, with a relatively high abundance, namely 12–20% relative to H_2O ice (de Graauw et al. 1996, d'Hendecourt et al. 1996, Gürtler et al. 1996, Whittet et al. 1998). In addition to solid CO_2 several other ice components could be identified in protostars. Solid CH_4 was detected with an abundance of ∼1–4% and OCS with an abundance of 0.04–0.2% relative to H_2O ice toward protostars (Boogert et al. 1996, Dartois et al. 1998, Palumbo et al. 1995,1997). ISO observations of CO_2 and CH_4 in the gas phase indicate low abundances (Dartois et al. 1998, van Dishoeck et al. 1996, van Dishoeck 1998, Boogert et al. 1998). Observations of the 6 μm absorption band of NGC7538 IRS9 by ISO-SWS showed that this feature cannot be matched using only the OH bending mode of H_2O ice. A good match was obtained by adding

the carbonyl C=O stretching mode absorption of organic acids, specifically formic acid (Schutte et al. 1996).

Recent ISO observations indicate that H_2O, CO_2 and CH_3OH ices dominate the grain surface close to massive protostars, where volatile ices are already sublimed (Gerakines et al. 1999, Boogert et al. 1999a). Extensive ice segregation involving CO_2 and CH_3OH was observed in the protostellar environment and is currently used as a sensitive tracer to investigate the evolution of ices in such environments (Ehrenfreund et al. 1998). It has been shown that solid CH_3OH and CO_2 exhibit specific intermolecular interactions which can be readily identified with infrared spectroscopy (Dartois et al. 1999b).

In this paper we present a database of laboratory studies of ice mixtures dominated by CO_2, CH_3OH and H_2O. We report the results of CO_2 in polar mixtures and focus on the intermolecular interactions monitored during annealing, in order to constrain the processes occurring during ice segregation. This extends earlier studies of laboratory ice analogs containing CO_2 in apolar ices (Ehrenfreund et al. 1996a, 1997). Infrared spectroscopic studies on CO_2 and CH_3OH ices have been previously performed by a number of authors. Sandford & Allamandola (1990) studied the spectral properties of solid CO_2 in apolar and polar ices. The physical and spectral properties of annealed ices containing CH_3OH were studied by Sandford & Allamandola (1993). Palumbo et al. (1998) investigated the effects of annealing and ion irradiation on the bands of solid CO_2 mixed in apolar and polar ices. Recent studies of solid CH_3OH infrared band profiles in ion irradiated ices have been reported by Palumbo et al. (1999).

In Sect. 3.1 we discuss the spectroscopic characteristics of binary ices containing CO_2 and CH_3OH. In Sect. 3.2 we add H_2O to these binary mixtures and study the infrared spectrum. In Sect. 3.3 we discuss the stability of ice mixtures containing CO_2 and CH_3OH against UV radiation. The discussion of the results is presented in Sect. 4. The laboratory point of view is discussed in Sect. 4.1.1 and the observational constraints in Sect. 4.1.2. In Sect. 4.2 we report additional evidence for ice segregation in the ISM and in Sect. 4.3 we summarize the current view of the evolution of icy grains according to the new laboratory results.

2. Experimental

Ices were condensed as pure gas or gas mixtures in a high vacuum chamber on the surface of a CsI window, cooled by a closed cycle He refrigerator to 10 K. Gases and gas mixtures have been prepared in a glass vacuum manifold. The purity of the used compounds are as follows: H_2O(liquid), triply distilled; CO_2(gas), Praxair, 99.996%; CH_3OH(liquid), Janssen Chimica 99.9%. The deposition rate and sample thickness growth rate were about 10^{15} molec·cm^{-2}·s^{-1} and 1 μm·hr^{-1}, respectively. Infrared transmission spectra were obtained with a BioRad FTS 40A spectrometer at a resolution of 1 cm^{-1}. Stepwise annealing in temperature intervals of a few Kelvin showed substantial changes in the infrared spectra. Thermal processing was performed in a careful and slow manner to avoid local explosive sublimation of the ices. UV irradiation was performed using a
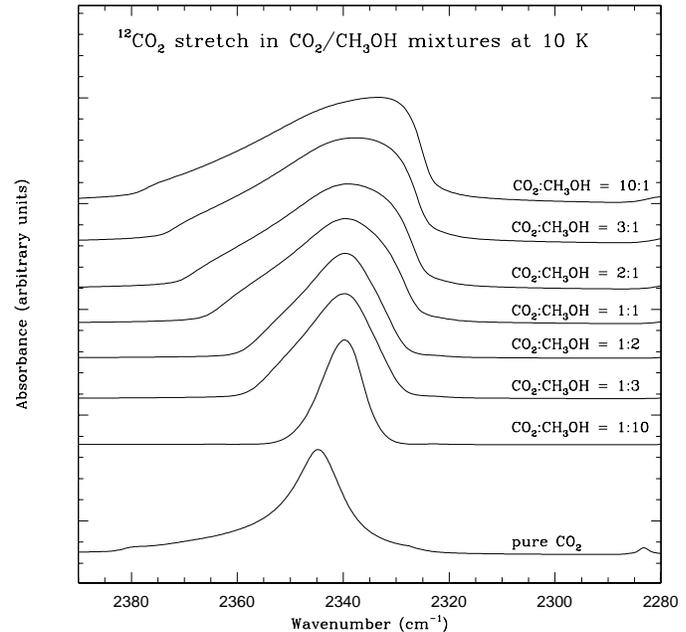

Fig. 1. Infrared absorption spectra of the $^{12}CO_2$ stretch in CO_2/CH_3OH mixtures at 10 K. Addition of 10% CH_3OH to CO_2 strongly broadens the band (FWHM of 37 cm^{-1}) and results in a redshift of about 10 cm^{-1}. Increasing the amount of CH_3OH shows a decrease in band widths of the CO_2 band. The band shifts at the same time toward higher frequencies. The difference in band position and width between CO_2:CH_3OH = 3:1 and 1:3 shows that the interactions between CH_3OH and CO_2 are strongly related to their abundance ratio and that a higher abundance of CO_2 (see Table 1) leads to stronger perturbation (and aggregate formation) reflected in a large band width.

microwave-excited hydrogen flow lamp. This source has a sharp emission peak at 1216 Å (Lyman α) and additional bands centered at 1360, 1450, 1600 and 2800 Å , which produce a total UV flux of approximately 10^{15} photons·cm^{-2}·s^{-1} (Weber & Greenberg 1985). Values for the infrared cross sections have been taken from Gerakines et al. (1995) for H_2O and CO_2 and from Kerkhof et al. (1999) for CH_3OH.

3. Results

3.1. CO₂/CH₃OH binary mixtures

3.1.1. CO₂ ice

The spectrum of solid CO_2 shows a strong stretching mode at 2342 cm^{-1} (4.27 μm) which was recently detected ubiquitously in the dense interstellar medium with the ISO satellite (de Graauw et al. 1996). Also the isotope $^{13}CO_2$, situated at 2280 cm^{-1} (4.38 μm), was detected with ISO, allowing the estimation of the carbon isotope ratio in the Galaxy (Boogert et al. 1999a). The other active infrared bands of solid CO_2 are the bending mode at 650 cm^{-1} (15.2 μm) and the combination modes at 3700 cm^{-1} (2.70 μm) and 3600 cm^{-1} (2.78 μm), respectively.

Fig. 1 shows the stretching mode of $^{12}CO_2$ in binary mixtures with CH_3OH at 10 K. Surprisingly, at concentrations of
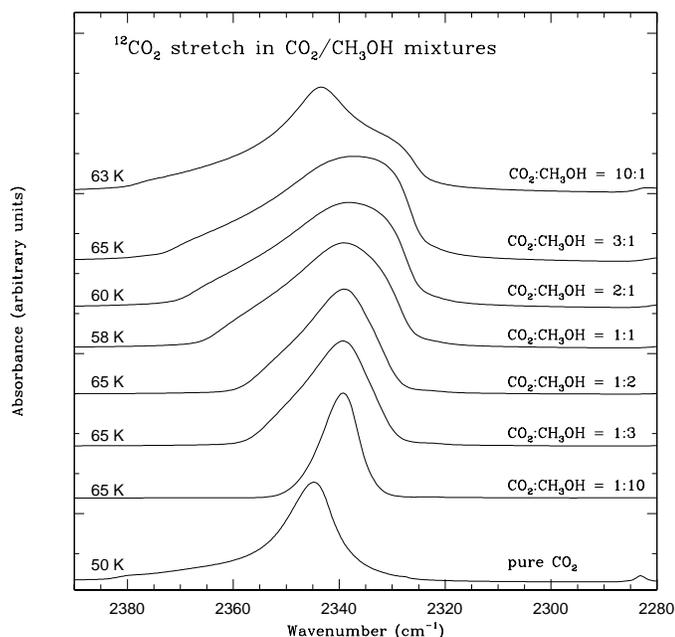
Fig. 2. Infrared absorption spectra of the $^{12}CO_2$ stretch in CO_2/CH_3OH mixtures at ~ 60 K. All spectra show exactly the same profile as the 10 K measurements (compare Fig. 1). Only the CO_2:CH_3OH = 10:1 mixture shows a change in profile. This mixture is rather volatile and the ice matrix is rearranged at low temperatures.

Fig. 3. Infrared absorption spectra of the $^{12}CO_2$ stretch in a CO_2:CH_3OH = 1:1 mixture during warm-up to 125 K. At 10 K we observe a single peak centered at $\sim 2340\,cm^{-1}$ which is characterized by a large band width of $26\,cm^{-1}$. During warm-up a second peak starts to arise and becomes dominant at 125 K. As comparison we show pure CO_2 centered at $2345\,cm^{-1}$ with a band width of $12\,cm^{-1}$.

10% CH_3OH diluted in CO_2 ice, the spectrum of the CO_2 stretch shows a band width of $37\,cm^{-1}$, the largest ever measured for this feature. Large band widths are also observed in mixtures of CO_2 and H_2O when CO_2 dominates (Ehrenfreund et al. 1997). H_2O-CO_2 interactions have been studied in nitrogen matrices and indicate that those molecules form a 1:1 complex where the C_2 axis of H_2O is orthogonal to the CO_2 molecule, with the O of H_2O pointing toward the CO_2 carbon (Fredin & Nelander 1976). An explanation for the large band width in CO_2:CH_3OH mixtures might be that CO_2 molecules encage CH_3OH molecules and form a unique structure in the ice. CO_2 mixtures which contain small amounts of H_2O or CH_3OH show, in addition to the large band width, a strong redshift to $2330\,cm^{-1}$. The band width decreases when the CH_3OH concentration is enhanced (see Fig. 1). Spectroscopic studies of CO_2 in Argon matrices indicate a feature around $2333\,cm^{-1}$ which is ascribed to CO_2 polymers, dimers and monomers (van der Zwet et al. 1989). This indicates that the wing at $2330\,cm^{-1}$ may have a similar origin. During warm-up of the mixture CO_2:CH_3OH = 10:1 to ~ 60 K the ice structure is rearranged and a band similar to pure CO_2 becomes visible. Only the red shoulder indicates the remaining interaction between CO_2 and CH_3OH (see Fig. 2).

Fig. 3 shows the CO_2 stretching mode during warm-up in a mixture of CO_2:CH_3OH = 1:1. The band position of the CO_2 stretch in such a mixture is relatively close to pure CO_2 but the width is twice as large. During the annealing process the band shows a strong change in the profile, indicating that CO_2 and CH_3OH strongly interact.
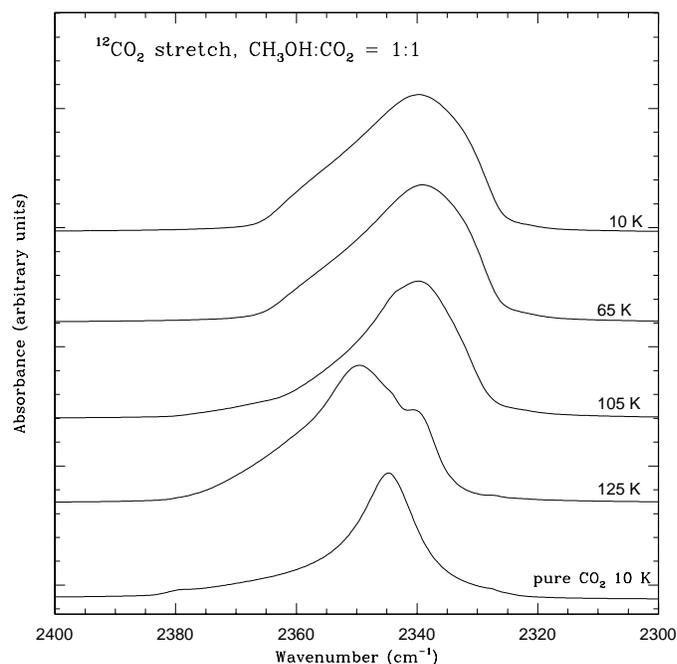
Strong complexes between CH_3OH and CO_2 are evident in the CO_2 bending mode displayed in Fig. 4. At 10 K only pure CO_2 shows a narrow and pronounced double peak at $660\,cm^{-1}$ and $655\,cm^{-1}$ ($15.2\,\mu m$ and $15.3\,\mu m$) due to the degeneracy of the transition. The addition of CH_3OH in the ice produces a broad second peak centered at $648\,cm^{-1}$ ($15.4\,\mu m$). Warm-up to 60 K shows changes only in the most volatile mixture, namely CO_2:CH_3OH = 10:1. Warm-up to higher temperatures >100 K shows the formation of double and triple-peak structures for the CO_2 dominated mixtures. We discuss the CO_2 bending mode in detail in Sect. 3.2. The spectroscopic characteristics of the $^{12}CO_2$ stretching mode, the $^{13}CO_2$ stretching mode and the $^{12}CO_2$ bending mode in 30 different mixtures are listed in Table 1.

3.1.2. CH_3OH ice

The spectrum of CH_3OH shows a wealth of bands in the near and mid-infrared region (Sandford & Allamandola 1993). The infrared CH stretching modes and the combination modes of CH_3OH, as well as the strong CO stretching mode of CH_3OH have been measured and are listed in Table 2. In Fig. 5 we display the CH stretching modes of CH_3OH in binary mixtures with CO_2.

The mixture CO_2:CH_3OH = 10:1 shows very sharp features. By increasing the CH_3OH concentration the ν_9 CH stretching modes of CH_3OH merge into a broad feature due to H-bonding.

Table 1. Positions and widths (in cm^{-1}) of $^{12}CO_2$ and $^{13}CO_2$ infrared absorption features in binary and multicomponent ice mixtures. (s) indicates band shoulders.

Ice composition	$^{12}CO_2$ stretch		$^{13}CO_2$ stretch		$^{12}CO_2$ bend	
	Position cm^{-1}	FWHM cm^{-1}	Position cm^{-1}	FWHM cm^{-1}	Position cm^{-1}	FWHM cm^{-1}
H_2O:CO_2=10:1	2342.4	16.7	2277.9	8.8	653.6/	28.6
H_2O:CO_2=1:1	2338.4	34.3	2279.3	8.6	655.2	27.6
CO_2:CH_3OH=10:1	2333.5	37.2	2279.2	8.4	655.5	15.5
CO_2:CH_3OH=3:1	2337.8	34.3	2277.8	8.9	656.4/641.8(s)	20.9
CO_2:CH_3OH=2:1	2339.1	31.1	2277.0	8.3	657.0/643.1(s)	24.8
CO_2:CH_3OH=1:1	2339.8	25.7	2276.1	7.4	658.3/647.5	13.1/20.3
CO_2:CH_3OH=1:2	2339.6	18.4	2275.2	6.7	658.2(s)/646.1	11.6/23.4
CO_2:CH_3OH=1:3	2339.8	16.9	2275.1	6.6	657.2(s)/645.8	10.6/22.8
CO_2:CH_3OH=1:10	2339.8	10.0	2274.6	5.8	656.7(s)/644.7	28.0
H_2O:CH_3OH:CO_2=90:10:20	2342.0	19.4	2277.9	8.4	653.0	29.7
H_2O:CH_3OH:CO_2=20:60:100	2339.6	28.2	2276.9	7.8	657.3/644.6(s)	29.3
H_2O:CH_3OH:CO_2=40:60:100	2339.7	28.4	2277.2	7.8	656.9/645.2(s)	28.5
H_2O:CH_3OH:CO_2=100:60:100	2340.9	25.7	2277.5	7.9	656.4/645.9(s)	28.3
H_2O:CH_3OH:CO_2=50:70:100	2341.3	25.6	2277.1	7.9	657.5/645.8(s)	31.9
H_2O:CH_3OH:CO_2=80:90:100	2341.3	24.0	2276.9	8.4	657.7/646.8	14.9/21.6
H_2O:CH_3OH:CO_2=100:100:100	2341.4	24.3	2277.1	7.7	657.8/644.6(s)	33.7
H_2O:CH_3OH:CO_2=70:100:100	2341.2	23.6	2276.7	7.7	658.1/649.6	14.0/21.4
H_2O:CH_3OH:CO_2=60:100:80	2341.1	21.6	2276.3	7.2	659.2/648.8	13.3/23.7
H_2O:CH_3OH:CO_2=120:70:100	2342.2	26.0	2277.8	7.9	657.3	32.3
H_2O:CH_3OH:CO_2=70:90:100	2341.3	24.9	2277.2	7.8	658.0	31.8
H_2O:CH_3OH:CO_2=50:100:100	2339.4	21.6	2276.6	7.6	654.8/648.6	19.1/23.2
H_2O:CH_3OH:CO_2=90:140:100	2339.3	19.8	2276.0	7.6	658.6/647.3	10.9/18.9
H_2O:CH_3OH:CO_2=20:50:100	2337.8	26.6	2277.5	8.2	656.9/643.7(s)	24.7
H_2O:CH_3OH:CO_2=30:50:100	2337.6	27.0	2277.5	8.1	649.9/643.6(s)	24.6
H_2O:CH_3OH:CO_2=30:70:100	2339.0	24.1	2276.9	8.0	657.4/649.3(s)	14.0/15.4
H_2O:CH_3OH:CO_2=110:120:100	2341.9	21.8	2277.1	7.8	656.7	33.8
H_2O:CH_3OH:CO_2=90:30:100	2341.8	29.7	2276.8	8.4	656.4	31.1
H_2O:CH_3OH:CO_2:NH_3=70:70:100:70	2341.6	24.4	2277.1	7.4	658.3/649.4(s)	14.3/18.8
H_2O:CH_3OH:CO_2:CH_4=60:70:100:10	2341.0	26.4	2276.8	7.3	657.9/650.2(s)	15.0/15.8
H_2O:CH_3OH:CO_2:CH_4=40:60:100:23	2340.5	25.8	2288.5	7.2	658.1/649.6(s)	13.5/16.2

The ν_3 CH stretching mode is rather stable in band position and band width in all the displayed mixtures.

Fig. 6 shows distinct differences for the ν_4, ν_5, ν_6, ν_{10} CH$_3$ deformation modes of CH_3OH around 1460 cm^{-1} at various mixing ratios with CO_2 in pure CH_3OH ice. The deformation mode consists of three narrow peaks at $\sim$1475 cm^{-1}, 1465 cm^{-1} and 1447 cm^{-1} and a broad shoulder at $\sim$1420 cm^{-1}. Upon dilution with CO_2 additional bands appear at 1380 cm^{-1}, 1340 cm^{-1} and 1276 cm^{-1}. The bands at 1380 cm^{-1} and 1276 cm^{-1} are attributed to infrared inactive CO_2 modes which are activated by perturbing interactions with neighbouring molecules. We compared these inactive CO_2 bands in the mixture CO_2:CH_3OH = 1:1 with the CO_2 stretch and derived their band strengths; $1.4 \cdot 10^{-20}$ cm·molecule^{-1} for the 1380 cm^{-1} band and $\leq 6.9 \cdot 10^{-21}$ cm·molecule^{-1} for the 1276 cm^{-1} band. The band strength increase in the mixture CO_2:CH_3OH = 10:1 is $\sim 1.8 \cdot 10^{-20}$ cm·molecule^{-1} and $\sim 9.0 \cdot 10^{-21}$ cm·molecule^{-1} for the 1380 and 1276 cm^{-1} features, respectively. The peak at 1340 cm^{-1} is ascribed to CH_3OH isolated in the apolar CO_2 matrix. The appearence

of this feature upon increasing dilution with CO_2 coincides with the growth of a feature at 3634 cm^{-1}. This latter band can be clearly ascribed to the OH stretching mode of CH_3OH monomers or dimers in an apolar matrix. The isolation causes a strong blueshift of the feature relative to the position in the fully H-bonded network. This behaviour is very analogues to that observed for the OH stretching mode of H_2O in apolar matrices (Ehrenfreund et al. 1996b).

For gas phase CH_3OH the ν_6 transition splits in two features at 1339 cm^{-1} and 1332 cm^{-1}, respectively (Serrallach et al. 1974). Thus the 1340 cm^{-1} band falls very close to the gas phase position of the ν_6 band, confirming the assignment to isolated CH_3OH. We compared the 1340 cm^{-1} band in the mixture CO_2:CH_3OH = 1:1 with the CO stretch in CH_3OH and derived the bandstrength (per molecule CH_3OH): $1.2 \cdot 10^{-20}$ cm·mol^{-1}. This value is dramatically enhanced by a factor of 280 in the CO_2:CH_3OH = 10:1 mixture, resulting in a band strength of $3.2 \cdot 10^{-18}$ cm·molecule^{-1}.

Table 2. Position and widths (in cm^{-1}) of CH_3OH infrared absorption features in binary and multicomponent ice mixtures. (s) indicates band shoulders.

| Ice composition | CH_3OH CO stretch | | CH_3OH CH stretch (ν_3) | | CH_3OH combinations |
	Position cm^{-1}	FWHM cm^{-1}	Position cm^{-1}	FWHM cm^{-1}	Position cm^{-1}
CO_2:CH_3OH=10:1	1020.8	26.4	2847.3	29.8	2668.9/2611.1
CO_2:CH_3OH=3:1	1025.1	31.6	2835.3	42.0	2590.3/2529.0
CO_2:CH_3OH=2:1	1025.8	31.6	2834.2	43.0	2590.0/2526.0
CO_2:CH_3OH=1:1	1025.7	32.6	2831.4	42.2	2591.6/2526.9
CO_2:CH_3OH=1:2	1025.8	32.3	2829.7	40.3	2592.8/2528.0
CO_2:CH_3OH=1:3	1026.0	32.2	2829.4	40.5	2591.9/2527.5
CO_2:CH_3OH=1:10	1026.1	31.0	2827.9	32.3	2592.0/2528.2
H_2O:CH_3OH:CO_2=90:10:20	1015.9	27.3	2833.5	38.9	2600.6/2542.6
H_2O:CH_3OH:CO_2=20:60:100	1024.9	32.5	2833.7	45.7	2592.1/2528.3
H_2O:CH_3OH:CO_2=40:60:100	1023.0	33.2	2833.7	44.4	2592.5/2531.4
H_2O:CH_3OH:CO_2=100:60:100	1018.7	33.5	2833.2	46.6	2597.3/2536.7
H_2O:CH_3OH:CO_2=50:70:100	1023.5	35.1	2832.5	42.6	2593.5/2532.4
H_2O:CH_3OH:CO_2=80:90:100	1024.1	35.5	2832.0	45.7	2594.0/2533.5
H_2O:CH_3OH:CO_2=100:100:100	1023.7	35.5	2832.3	44.7	2594.2/2534.4
H_2O:CH_3OH:CO_2=70:100:100	1025.1	35.3	2831.7	44.2	2593.6/2531.5
H_2O:CH_3OH:CO_2=60:100:80	1025.8	35.2	2831.1	43.7	2592.4/2531.3
H_2O:CH_3OH:CO_2=120:70:100	1022.2	35.4	2832.6	49.4	2597.7/2535.9
H_2O:CH_3OH:CO_2=70:90:100	1025.3	35.5	2831.6	45.0	2595.5/2532.6
H_2O:CH_3OH:CO_2=50:100:100	1019.3	33.5	2758.6	45.0	2594.3/2528.9
H_2O:CH_3OH:CO_2=90:140:100	1025.0	32.7	2830.0	43.3	2594.5/2530.8
H_2O:CH_3OH:CO_2=20:50:100	1025.8	32.2	2833.4	45.2	2595.4/2527.7
H_2O:CH_3OH:CO_2=30:50:100	1026.2	32.3	2833.7	44.9	2591.2/2529.9
H_2O:CH_3OH:CO_2=30:70:100	1025.2	33.1	2832.9	43.4	2594.3/2529.7
H_2O:CH_3OH:CO_2=110:120:100	1024.2	36.4	2831.8	41.6	2596.1/2536.4
H_2O:CH_3OH:CO_2=90:30:100	1018.7	31.1	2834.1	51.5	2599.0/2538.4
H_2O:CH_3OH:CO_2:NH_3=70:70:100:70	1026.9	30.9	2827.2	43.8	2618.4/2594.4(s)/2537.6
H_2O:CH_3OH:CO_2:CH_4=60:70:100:10	1024.6	33.4	2832.2	39.0	2593.0/2532.8
H_2O:CH_3OH:CO_2:CH_4=40:60:100:23	1025.1	33.1	2832.5	40.4	2595.9/2531.1

3.2. H_2O/CO_2/CH_3OH mixtures

Parameters of the CH_3OH and CO_2 bands in mixtures to which H_2O has been added are included in Tables 1 and 2. Fig. 7 shows the CO_2 stretching mode during warm-up in a mixture of H_2O, CH_3OH and CO_2 in equal proportions. The band position of the CO_2 stretch in such a mixture is relatively close to pure CO_2 but the width is twice as large. During the annealing process the band shows strong changes in the profile, indicating that the three molecules strongly interact.

In Fig. 8 we show the bending mode which appears rather broad at 10 K ($\sim$34 cm^{-1}). During the warm-up a triple-peak structure is formed. Whereas the double peak has been discussed by Ehrenfreund et al. (1996a), the shoulder at 648 cm^{-1} (15.4 μm) has been identified with CO_2-CH_3OH complexes (Ehrenfreund et al. 1998, Dartois et al. 1999b). Warming up to even higher temperatures of 120 K in the laboratory gives a double peak profile. The triple-peak is stable in laboratory spectra during a temperature interval of $\sim$15–40 K depending on the exact ice composition. In comparison with binary mixtures of CO_2 and CH_3OH, addition of H_2O enhances the temperature interval over which the triple-peak is stable by $\sim$250% and also decreases the width by $\sim$10%. The shoulder at 648 cm^{-1}

(15.4 μm) disappears only at higher temperature, at which the 665 cm^{-1} (15.0 μm) peak becomes broad and dominant. The shoulder is produced by the Lewis acid-base interaction between the carbon atom of CO_2 and the oxygen atom of a specific polar molecule such as CH_3OH (Dartois et al. 1999b). Polar molecules such as H_2O and NH_3 in abundance inhibit the complex formation due to their efficient hydrogen bonding ability (Dartois et al. 1999b).

Fig. 9 shows the effect of the CH_3OH concentration on the profile of the CO_2 bending mode at $T\sim$105 K. The shoulder at 648 cm^{-1} (15.4 μm) increases when the CH_3OH concentration increases. The triple peak structure remains after recooling to 10 K. For a detailed chemical view of the molecular complexes in such ices and their chemical properties the reader is referred to Dartois et al. (1999b).

The effect of the varying H_2O content on the profile of the CO_2 bending mode is displayed in Fig. 10 which shows a comparison of laboratory measurements with each other and with astronomical data of the massive protostar W33A. The astrophysical implications will be discussed in Sect. 4. A water dominated mixture does not show a multipeak structure upon thermal processing. When the H_2O content becomes compara-
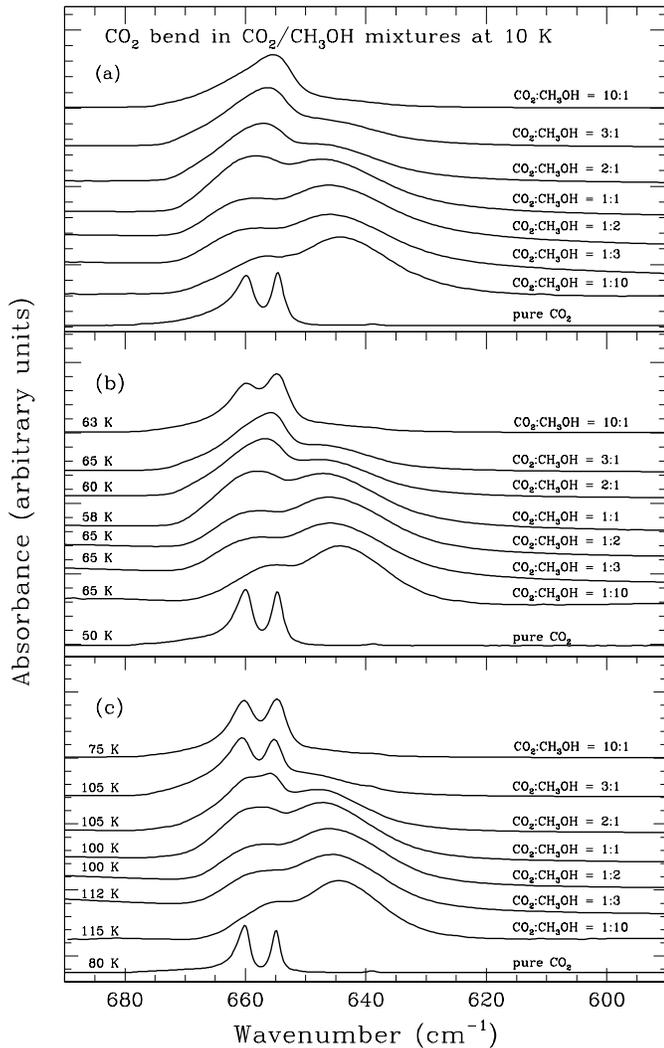
Fig. 4a–c. Infrared absorption spectra of the CO_2 bending mode in CO_2/CH_3OH mixtures at 10 K, ∼60 K and ∼100 K. In pure CO_2 the spectrum of the bending mode shows a double peak at 660 cm^{-1} and 655 cm^{-1}, respectively. **a** At 10 K the addition of 10% CH_3OH shows a single peak at 655 cm^{-1}. When increasing the CH_3OH content in the mixture, a second peak appears at ∼ 648 cm^{-1} due to the formation of complexes. **b** At temperatures of ∼60 K we observe the same behavior. The 10% CH_3OH mixture shows a double peak indicating interaction between CO_2 molecules in the ice segregation process. **c** At temperatures of ∼ 100 K we observe peak splitting for mixtures where CO_2 is abundant. CH_3OH-dominated mixtures show similar profiles for all temperatures, due to their higher stability during thermal processing.
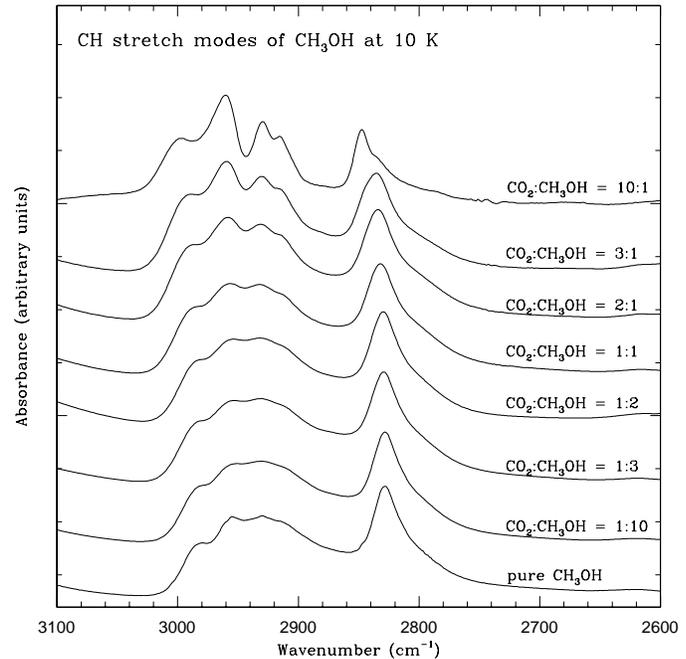

Fig. 5. Infrared absorption spectra of the CH stretching modes of solid CH_3OH mixed with CO_2. For the ν_9 stretch 4 peaks centered around 2960 cm^{-1} are observed. The narrow band at positions varying between 2847 cm^{-1} and 2827 cm^{-1} corresponds to the ν_3 stretch. The latter shifts toward lower frequencies as the CO_2/CH_3OH ratio decreases (see also Table 2). At the same time the multipeak structure of the ν_9 stretch at 2950 cm^{-1} (3.39 μm) becomes less pronounced.

$^{13}CO_2$ stretch in the laboratory and in the ISM see Boogert et al. (1999a).

In Fig. 12 we show the OH stretching mode of H_2O and CH_3OH in an H_2O:CH_3OH:CO_2 = 1:1:1 mixture during warm-up. During warm-up to 136 K the OH stretching mode which falls at 3290 cm^{-1} (3.0 μm) at 10 K shows a large redshift of 37 cm^{-1} and isolated H_2O and CH_3OH bands, visible at 10 K between 3700–3660 cm^{-1}, disappear. This indicates a re-arrangement of the H_2O and CH_3OH molecules in the ice ma-trix. The overtones of CO_2 at 3700 cm^{-1} and 3600 cm^{-1}, re-spectively, show a decrease in band width and a blueshift of ∼10 cm^{-1}, as observed for pure CO_2.

Fig. 13 displays the region of the H_2O bending mode at 1660 cm^{-1} (6.02 μm) and the CH_3OH deformation mode around 1460 cm^{-1} (6.8 μm) during annealing of a mixture H_2O:CH_3OH:CO_2 = 1:1:1. The deformation mode of CH_3OH consists of 4 peaks: three narrow peaks at ∼ 1477 cm^{-1}, 1462 cm^{-1} and 1450 cm^{-1} and a broad shoulder at ∼ 1420 cm^{-1} corresponding to the ν_4, ν_5, ν_6 and ν_{10} CH_3 de-formation modes. For the 1450 cm^{-1} peak we find a redshift of ∼ 5 cm^{-1} during warm-up, whereas the other bands are stable in position. The slope of the three narrow peaks is however in-versed during warm-up. The H_2O bend appears broad at 10 K and decreases in width during warm-up. At 112 K a second band develops at the blue wing at 1720 cm^{-1} (5.81 μm).

In Fig. 14 we show the CO stretching mode of CH_3OH at 10 K in various mixtures. The CO stretch is rather stable in

ble to CO_2 and CH_3OH, the band is shifted to the blue and the triple substructure starts to appear since CO_2 complexes with it-self and with CH_3OH are now able to form. Further lowering of the H_2O ice concentration (H_2O/CO_2<30%) causes a general redshift of the band and an enhancement of the broad 15.4 μm shoulder of CO_2-CH_3OH complexes.

Fig. 11 shows the $^{13}CO_2$ band in various mixtures contain-ing CH_3OH and H_2O. In all cases the $^{13}CO_2$ band is broad and shifted relative to pure CO_2. For a detailed discussion of the
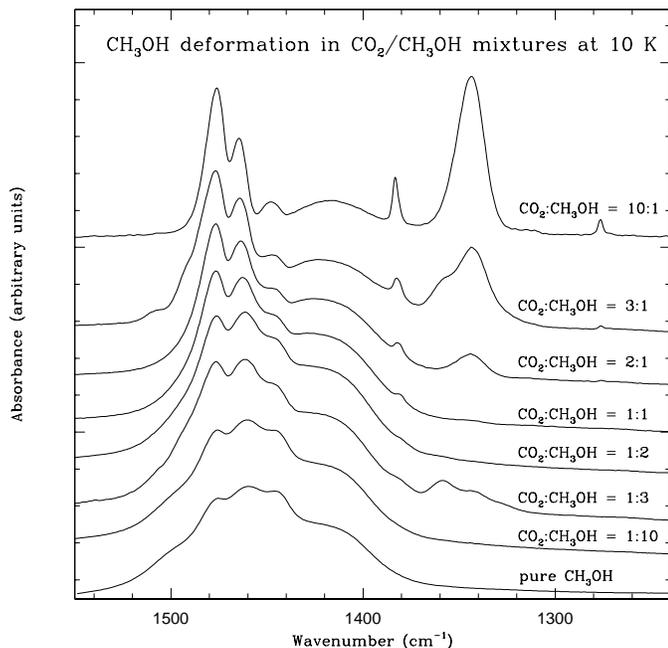
Fig. 6. Infrared absorption spectra of the CH$_3$OH deformation in CO$_2$/CH$_3$OH mixtures at 10 K. The deformation mode consists of three narrow peaks at $\sim$ 1475 cm^{-1}, 1465 cm^{-1} and 1447 cm^{-1} and a broad shoulder at $\sim$ 1420 cm^{-1}. The structure of the triple-peak smoothens as the relative amount of CH$_3$OH increases. The extra peaks at 1380 cm^{-1}, 1276 cm^{-1} and 1340 cm^{-1} are particularly strong in the mixture CO$_2$:CH$_3$OH = 10:1. They may be attributed to the infrared inactive CO$_2$ modes and isolated CH$_3$OH, respectively.

Fig. 7. Infrared absorption spectra of the ^{12}CO$_2$ stretch in a H$_2$O:CH$_3$OH:CO$_2$ = 1:1:1 mixture during warm-up up to 136 K. At 10 K we observe a single peak centered at $\sim$ 2341 cm^{-1} which is characterized by a large band width of 24 cm^{-1}. At 117 K a second peak starts to arise as a blue wing probably due to aggregate formation. With increasing temperature the 2341 cm^{-1} peak decreases in strength. As comparison we show pure CO$_2$ centered at 2345 cm^{-1} with a band width of 12 cm^{-1}.

position and width in the mixtures reported here. The band width varies between 26.4 cm^{-1} and 35.5 cm^{-1} and the band position varies between 1026 cm^{-1} and 1016 cm^{-1}. The peak appearing at 1080 cm^{-1} in CO$_2$:CH$_3$OH=10:1 likely corresponds to the CO stretching mode of CH$_3$OH isolated in the apolar matrix.

Finally Fig. 15 displays the combination modes of CH$_3$OH at 2600 (3.84 μm) and 2526 cm^{-1} (3.96 μm) at 10 K. These CH$_3$OH bands can be observed with ground based telescopes and are used to estimate CH$_3$OH abundances in the ISM. As shown in the figure, they are rather stable in shape in those mixtures. A strong blueshift is observed for mixtures with a low CH$_3$OH abundance compared to H$_2$O.

3.3. UV radiation

We have subjected CH$_3$OH-CO$_2$-H$_2$O mixtures to UV irradiation in order to study their stability in the protostellar environment. In Fig. 16 we display the destruction of CH$_3$OH and CO$_2$ in a H$_2$O:CH$_3$OH:CO$_2$ = 0.5:0.8:1.0 mixture at 10 K and 85 K. The thickness of the samples is less than 0.1 μm (see Sect. 2) to allow full penetration of UV photons. Also displayed is the destruction of CH$_3$OH in the pure phase. After 1 hour UV irradiation at 10 K the abundance of CH$_3$OH and CO$_2$ has decreased by 26% and 8% respectively and about twice as much after 2 hours irradiation. These values are rather low compared to 10 K measurements of pure ices, indicating that CH$_3$OH and CO$_2$
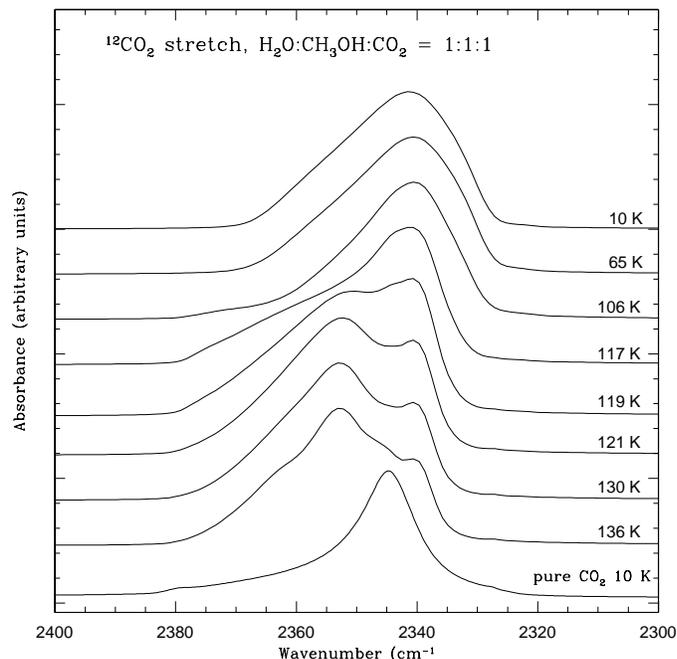
may be protected in such an amorphous ice structure. However, inherent instabilities in the lamp flux cannot be excluded and be partly responsible for differences in destruction rates. After 1 hour UV irradiation of the annealed ice mixture at 85 K we observe about 33% decrease of CO$_2$ as well as of CH$_3$OH. After 2 hours we measure a decrease of 60% of CH$_3$OH, CO$_2$ maintains at the same level because an equilibrium of formation and destruction is reached. Thus the annealed ice mixture is more vulnerable to UV photons, leading to faster destruction of CO$_2$ and CH$_3$OH.

In Fig. 17 we show the CO$_2$ bending mode of a H$_2$O:CH$_3$OH:CO$_2$ = 0.5:0.8:1.0 mixture at 10 K. The destruction of CH$_3$OH and CO$_2$ in such a mixture leads to the formation of CO, H$_2$CO and other photoproducts (cf. Gerakines et al. 1996). Only slight modifications in the CO$_2$ profile are observed after 2 hours of UV irradiation. In particular the shoulder around 648 cm^{-1} (15.4 μm) is diminishing over time. Since this peak is attributed to CH$_3$OH-CO$_2$ complexes, the efficient destruction of CH$_3$OH by UV light leads, obviously, to a decrease of this band.

Irradiating a mixture of H$_2$O:CH$_3$OH:CO$_2$=0.5:0.8:1.0 at 10 K does not produce a triple-peak structure. We also investigated the stability of this ice mixture, thermally processed to 85 K, by irradiating the annealed ice which displays the triple-peak structure in the CO$_2$ bend. This is shown in Fig. 18. After 1 hour UV irradiation the shoulder at 648 cm^{-1} (15.4 μm) has
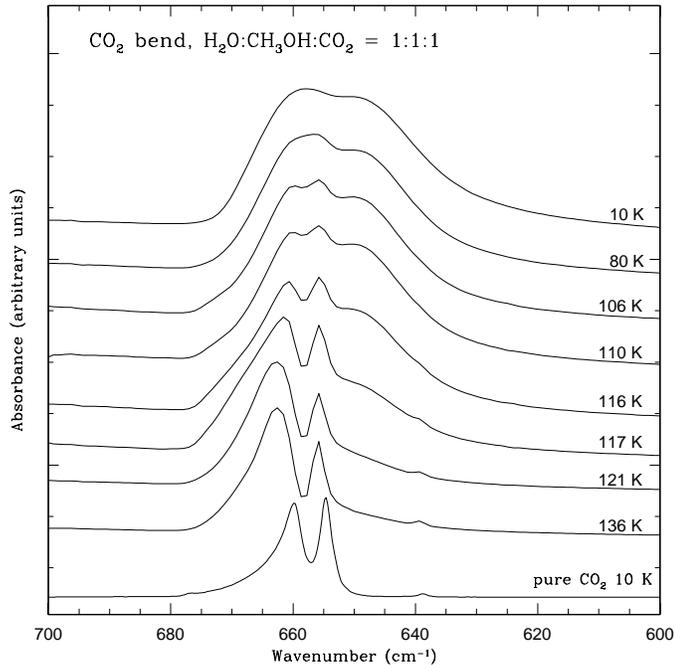
Fig. 8. Infrared absorption spectra of the CO_2 bending mode in an H_2O:CH_3OH:CO_2 = 1:1:1 mixture during annealing to 136 K. At 10 K the bending mode is characterized by a broad asymmetric profile with two shoulders at 658 cm^{-1} and 648 cm^{-1}. The peak at 658 cm^{-1} starts to split symmetrically at $\sim$90 K. The magnitude of the low frequency shoulder decreases with increasing temperature and disappears spontaneously at 121 K.

Fig. 9. Infrared absorption spectra of the CO_2 bending mode in annealed H_2O:CH_3OH:CO_2 mixtures. The profiles consist of two peaks at $\sim$ 660 cm^{-1} (15.15 μm) and 656 cm^{-1} (15.24 μm) and a shoulder at $\sim$ 648 cm^{-1} (15.4 micron). For increasing amounts of CH_3OH relative to H_2O and CO_2, this shoulder grows and becomes equal or larger than the other two peaks. This implies that the absorption at 648 cm^{-1} is due to complexes between CO_2 and CH_3OH (Ehrenfreund et al. 1998, Dartois et al. 1999b). A smaller abundance of H_2O enhances the shoulder at 15.4 μm and leads to an increased band width.

decreased significantly and cannot be observed any longer after 2 hours UV irradiation. This provides additional evidence that the 15.4 μm feature is due to CH_3OH-CO_2 complexes, which are destroyed by photolysis. In contrast, the double peak structure becomes more prominent with increased photolysis. Apparently, the photolysis stimulates the ice segregation process.

4. Discussion

4.1. Ice segregation

4.1.1. Amorphous versus crystalline H_2O – clathrates in the ISM?

Extensive and detailed studies of annealed binary and multiple ice mixtures containing CO_2, CH_3OH and H_2O allow us to monitor the motion of molecules and the overall changes in the ice matrix.

Recent ISO data display a very distinct triple-peak structure for the CO_2 bending mode (Gerakines et al. 1999). In comparison with laboratory results it was shown that the astronomical profile can only be reproduced when CH_3OH is added to CO_2 and H_2O ice. The best fit could be obtained using an annealed mixture of equal proportions of H_2O, CH_3OH and CO_2 (see Fig. 10). The shoulder at 648 cm^{-1} (15.4 μm), appearing during the annealing process has been identified with CO_2-CH_3OH complexes (Ehrenfreund et al. 1998, Dartois et al. 1999b). Warming up to even higher temperatures of 120 K in
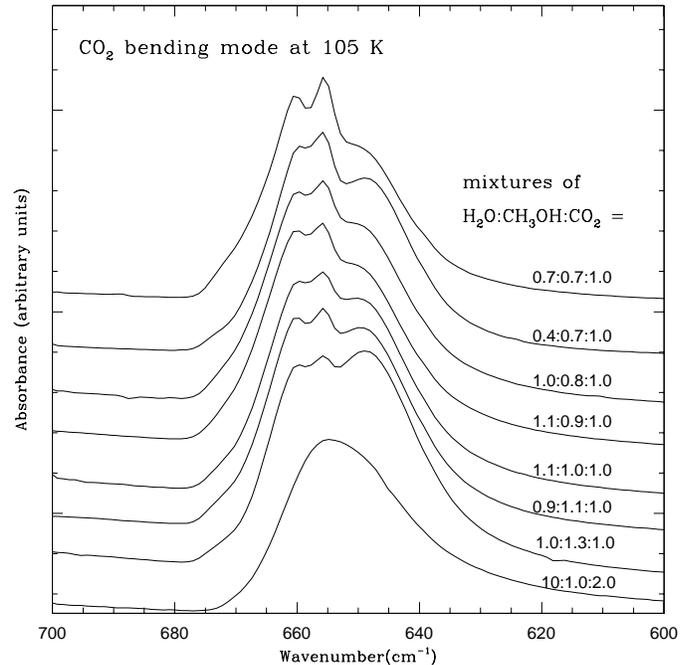
the laboratory gives a double peak profile, which is observed in warm protostellar regions such as S140 (Gerakines et al. 1999). The implications for the interpretation of astronomical data have been extensively discussed by Boogert et al. (1999a,b) and Gerakines et al. (1999).

Jenniskens & Blake (1994) defined with X-ray diffraction studies several structures of amorphous and crystalline H_2O ice. In cold dense clouds with temperatures of 10 K, H_2O ice exists apparently in the high density amorphous form. Conversion of H_2O ice from the high density amorphous to the low density amorphous form occurs in the laboratory between 38–68 K. During this phase the ice will rearrange and allow previously spatially separated species to interact. The presence of clathrate hydrates in cometary ices has been suggested to be responsible for gas releases at large radial distances from the Sun. Clathrate structures are nonstoichiometric solutions of small molecules within an ice-like H_2O network. CH_3OH as guest molecule in H_2O leads to the formation of type II clathrates. It has been shown that also CO_2 is capable of "stabilizing" the type II clathrate hydrate through interactions within the small cages (Fleyfel and Devlin 1991). The cubic type II clathrate hydrate is a polyhedral clathrate of $\sim$17 Å size. The unit cell contains H_2O molecules in a closest packing, linked together
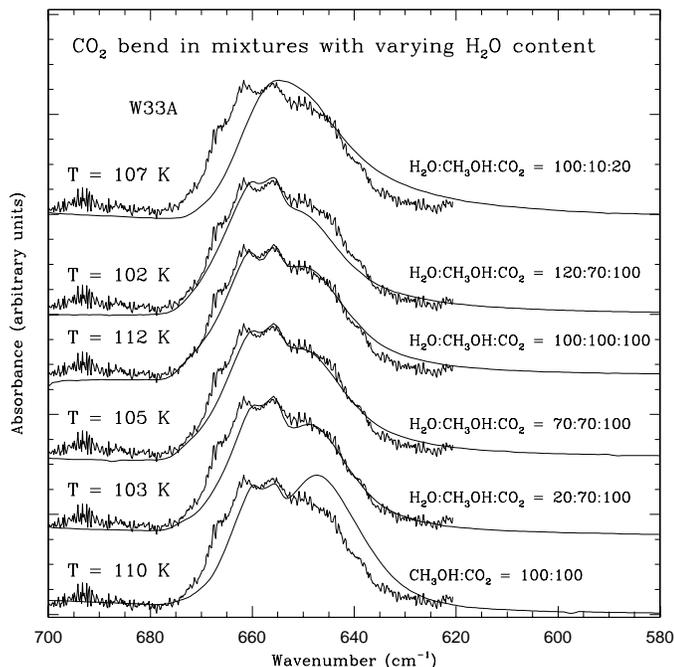
Fig. 10. Infrared absorption spectra of the CO_2 bending mode in annealed H_2O:CH_3OH:CO_2 mixtures with varying H_2O content ($H_2O/CO_2 = 0$–10) are compared to the spectrum toward the high mass protostar W33A. The best fit is obtained using a mixture with H_2O, CH_3OH and CO_2 in similar proportions. The shoulder at $\sim 667\,cm^{-1}$ is partly due to CO_2 gas in the line of sight of W33A.
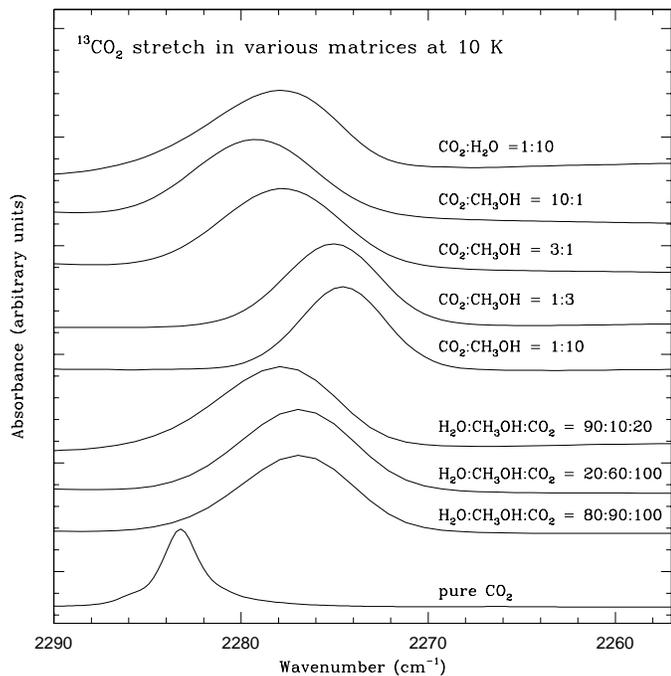

Fig. 11. Infrared absorption spectra of the $^{13}CO_2$ stretch in various matrices at 10 K. The addition of other molecules to CO_2 ice results in an increased band width varying between 5.8 and $9.8\,cm^{-1}$. The mixtures containing CH_3OH in abundance display a redshift of $\sim 8\,cm^{-1}$ compared to pure $^{13}CO_2$. Pure $^{13}CO_2$ is known to have a very narrow band width of $2.4\,cm^{-1}$.
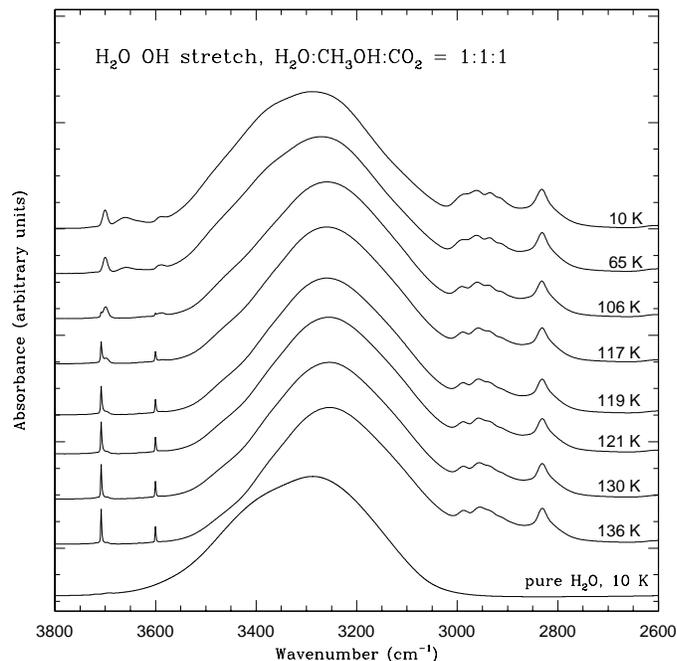

Fig. 12. Infrared absorption spectra of the OH stretching mode of H_2O at $3290\,cm^{-1}$ ($3.0\,\mu m$) in an H_2O:CH_3OH:$CO_2 = 1{:}1{:}1$ mixture during warm-up. Annealing to 136 K results in a redshift of the OH stretch of H_2O of $37\,cm^{-1}$. Isolated H_2O and CH_3OH bands around $3600\,cm^{-1}$ disappear during warm-up. The overtones of CO_2 at $3700\,cm^{-1}$ and $3600\,cm^{-1}$, blended at low temperature with isolated H_2O and CH_3OH bands, become sharper during warm-up and show a blueshift of $\sim 10\,cm^{-1}$. At the red wing of the $3.0\,\mu m$ band are the CH stretching modes of CH_3OH (see Fig. 5).

by hydrogen bonds, which can encage molecules of appropriate sizes (Mak & McMullan 1964).

Phase separations and microporous textures have been identified with electron microscopy in annealed H_2O-CH_3OH ices (Blake et al. 1991). Clathrate hydrates of type II have been unambiguously identified in mixtures where the ratio of the H_2O and guest molecule (CH_3OH) was as high as 2:1. The excess CH_3OH was segregated into grain boundary layers of nearly pure CH_3OH, which remained amorphous. In addition to the electron optical studies, Blake et al. (1991) recorded the infrared absorption spectra of H_2O-CH_3OH ices doped with a small amount of CO_2 to act as a sensitive local probe. During warming up to 125 K the $^{12}CO_2$ asymmetric stretching mode, peaked near $2340\,cm^{-1}$, was replaced by a blueshifted peak at $2346\,cm^{-1}$. The blue shift indicates that some of the CO_2 molecules were transferred into smaller, repulsive sites (Blake et al. 1991). These new sites were probably associated with the clathrate hydrate structure. We have observed a similar behavior of the $^{12}CO_2$ stretch profile during warm-up of H_2O:CH_3OH:$CO_2 = 1{:}1{:}1$ mixtures (see Fig. 7), which are however also observed in binary ice mixtures of CO_2 and CH_3OH without H_2O (see Fig. 3). An indication for the presence of "boundary phases" of pure ice could be the symmetric splitting of the CO_2 bending mode. The double-peak profile of the CO_2 bending mode in annealed multicomponent mixtures is much broader than the profile of pure
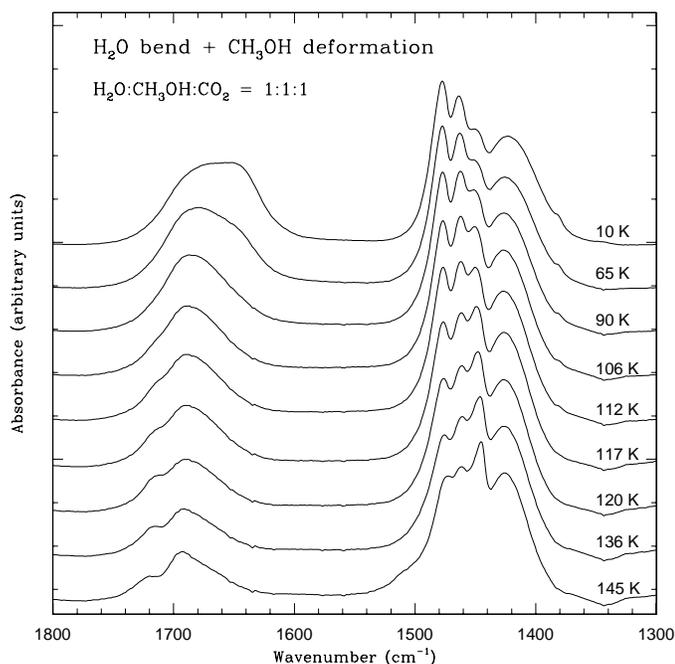
Fig. 13. Infrared absorption spectra of the H_2O bending mode and the CH_3OH deformation mode in a $H_2O:CH_3OH:CO_2 = 1:1:1$ mixture during warm-up. The deformation band of CH_3OH consists of 4 peaks: three narrow peaks at $\sim 1477\,cm^{-1}$, $1462\,cm^{-1}$ and $1450\,cm^{-1}$ and a broad shoulder at $\sim 1420\,cm^{-1}$. For the $1450\,cm^{-1}$ peak we find a redshift of $\sim 5\,cm^{-1}$ during warm-up, whereas the other bands are stable in position. The slope of the three narrow peaks is inversed during warm-up. The H_2O bend appears broad at 10 K and decreases in width during warm-up. At 112 K a second band developes at the blue wing at $1720\,cm^{-1}$ (5.81 μm).

Fig. 14. Infrared absorption spectra of the CO stretch in CH_3OH at 10 K. The band width varies between $26.4\,cm^{-1}$ and $35.5\,cm^{-1}$ and the position varies between $1026\,cm^{-1}$ and $1016\,cm^{-1}$.
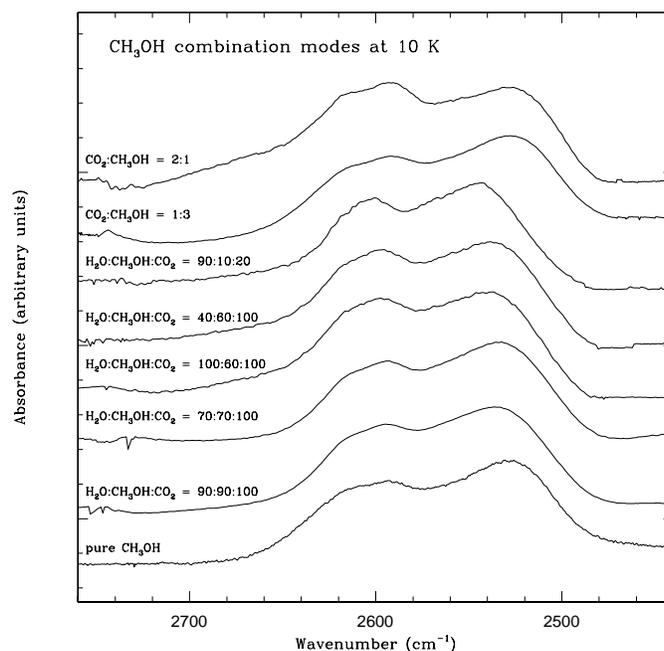

Fig. 15. Infrared absorption spectra of the combination modes of solid CH_3OH in various matrices containing also CO_2 and H_2O admixtures. The profile shape does not change significantly for the selected mixtures. A strong blueshift of $\sim 20\,cm^{-1}$ is observed in the mixture with high H_2O abundance.
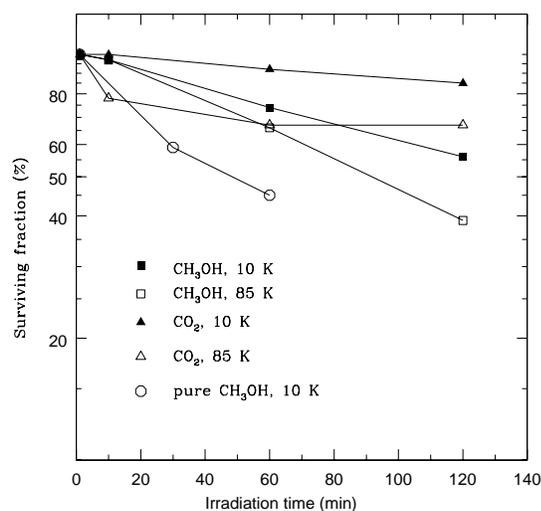

Fig. 16. Destruction of CH_3OH and CO_2 during irradiation of a $H_2O:CH_3OH:CO_2 = 0.5:0.8:1.0$ mixture at 10 K and after warm-up to 85 K. Also displayed is the destruction of pure CH_3OH.

CO_2 at 10 K. Spectroscopically we can also evidence that isolated H_2O and CH_3OH bands are strongly visible at 10 K but dissappear during the annealing process, probably joining the polymer (see Fig. 12).

To summarize, we have indications for the presence of clathrates and therefore evidence for partial crystallization of the ice. However, the described infrared properties may also result from changes in the ice matrix introduced during the conversion of high density amorphous ice to low density amorphous
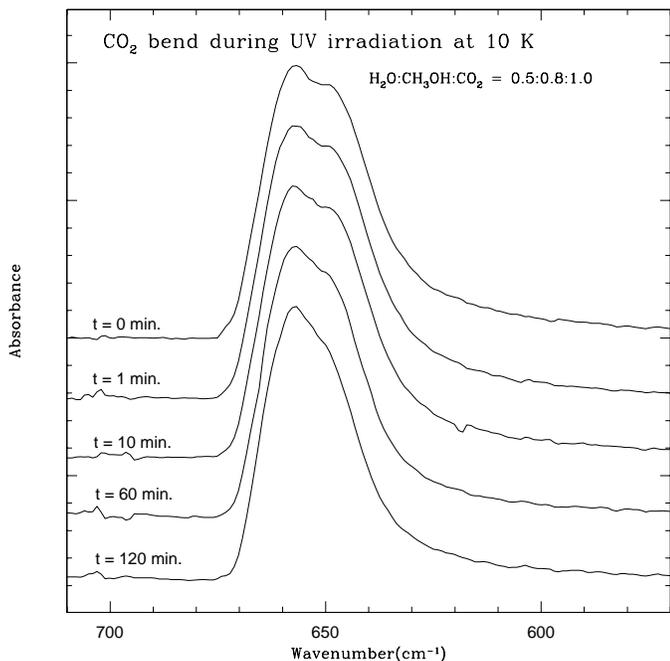
Fig. 17. Infrared absorption spectra of the CO_2 bending mode of a H_2O:CH_3OH:CO_2 = 0.5:0.8:1.0 ice mixture at 10 K during UV irradiation. After irradiation of two hours 44% of the CH_3OH and 15% of the CO_2 is destroyed and we observe a noticable decrease of the strength of the 648 cm^{-1} (15.4 μm) shoulder.
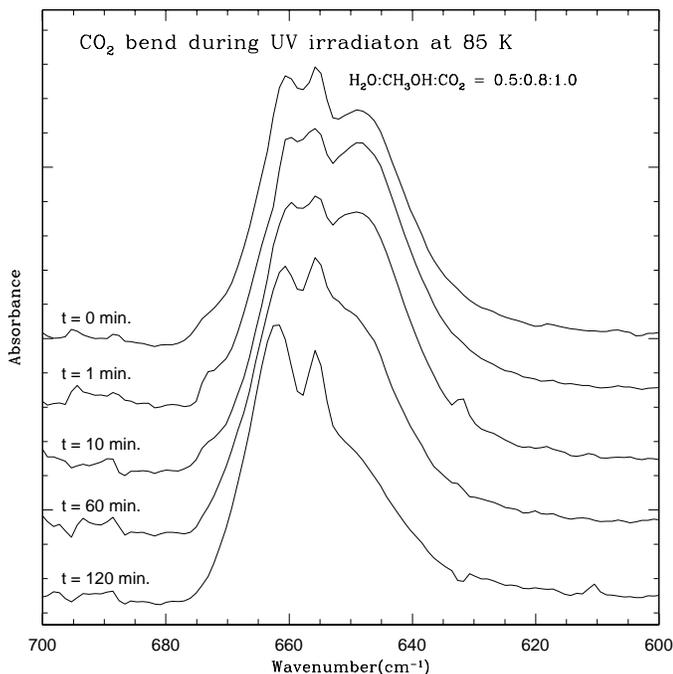

Fig. 18. Infrared absorption spectra of the CO_2 bending mode of an annealed H_2O:CH_3OH:CO_2 = 0.5:0.8:1.0 ice mixture displaying the triple peak. After two hours of UV irradiation 61% of the CH_3OH and 33% of the CO_2 is destroyed. The shoulder at 648 cm^{-1} completely vanishes and the peak splitting increases.

ice. Only X-ray diffraction studies can be conclusive about the ice structure during the annealing process.

4.1.2. Interstellar ice processing

Our current view of interstellar ices is that prior to the formation of the protostar rather volatile species accrete in an interstellar ice mantle. Observations of background field stars, probing cold dust in the general dense medium, show that the ice mantle in such regions is segregated in a polar and apolar ice phase (Sandford et al. 1988, Tielens et al. 1991, Chiar et al. 1998). This segregation may be caused by selective desorption events that separate the most volatile (CO, N_2) ice components, e.g. explosive mantle desorption or impulsive heating by cosmic rays (Léger et al. 1985, Schutte & Greenberg 1991). This then leads to an ice mantle showing a layered structure, i.e. with the stable refractory ices forming an inner mantle and the volatile ices on the outside. This layered ice mantle is thermally processed once the newly formed star warms up its environment. This then leads to a spatial separation of the ices. Far from the star where the temperatures are low, the initial volatile mantles survive and this can be recognized in the solid CO profile (Tielens et al. 1991, Chiar et al. 1998). Closer in, the more volatile species have evaporated, leaving behind H_2O, CH_3OH, and CO_2 in a mixed molecular ice along with the refractory ices (Ehrenfreund et al. 1998). Even closer in, these mixed ices segregate into separate ice components (but still on the same grain).

In this paper we have studied the spectroscopic properties of H_2O, CH_3OH and CO_2 ice mixtures at 10 K and during thermal processing and UV photolysis. The unique triple-peak structure of the CO_2 bending mode at 15.2 μm which was observed toward many sources in the interstellar medium could only be reproduced in the laboratory by adding significant amounts of CH_3OH to H_2O-CO_2 mixtures and subsequent thermal processing (Ehrenfreund et al. 1998). Annealed binary mixtures containing CH_3OH and CO_2 also show the triple-peak structure, but the overall position of the CO_2 bending mode is too red to fit the interstellar data (see Fig. 4 and Fig. 10). The H_2O molecules apparently play a fundamental role in stabilizing the CH_3OH-CO_2 complexes and the presence of H_2O shifts the CO_2 bend to obtain a perfect fit (see Fig 10). The annealed CO_2 band shows in the laboratory a stable profile over the temperature range 80–120 K, corresponding to $\sim$ 70–80 K in interstellar space (Boogert et al. 1999a). Complexes between CH_3OH and CO_2 lead to a shoulder at 15.4 micron which becomes too weak to fit the astronomical data when the H_2O exceeds the CH_3OH and CO_2 abundance by more than $\sim$ 20% (see Fig. 10). The abundances of CH_3OH and CO_2 have to be approximately equal in order to reproduce the triple-peak structure in astronomical data.

Any kind of processing, such as UV radiation, cosmic ray bombardment as well as cosmic ray induced UV radiation leads to the destruction of CH_3OH and CO_2. This in turn results in the destruction of the CH_3OH-CO_2 complexes and changes the CO_2 bending mode profile. The photolysis of annealed ice mixtures showed that this ice structure has a limited lifetime. We note
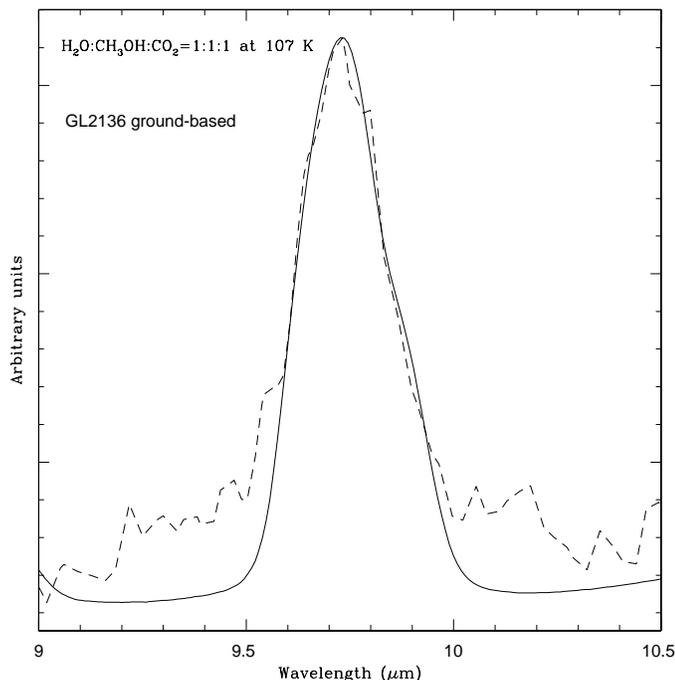
Fig. 19. The CO stretch of CH_3OH at $9.7\,\mu m$ ($1026\,cm^{-1}$) observed toward the YSO AFGL 2136 by Skinner et al. (1992) (dashed line) and a H_2O-CH_3OH-CO_2 mixture (solid line) in equal proportions, annealed to 107 K. The good fit indicates ice segregation and that CH_3OH is not mixed with the bulk of H_2O ice on grain mantles in the line-of-sight. The same mixture at 10 K does not fit these observations. The wings in the astronomical spectrum arise from smoothing the substantial noise at the continuum.

however that at the present time it is not possible to derive a strict quantitative upper limit for the irradiation dose, since this will strongly depend on the initial quantity of CH_3OH in the ice (i.e., before irradiation). In this context it should be noted that in some lines of sight the abundance of solid CH_3OH can exceed that of solid CO_2 by as much as a factor 1.4 (Dartois et al. 1999a). Using such high initial CH_3OH abundances would allow very significant UV processing equivalent to $\sim$2 hour of irradiation in the laboratory, i.e. a UV dose of 10^{19} photons·cm^{-2}, before the amount of solid CH_3OH would become too low to support the observed strong shoulder in the CO_2 bending mode due to the CO_2-CH_3OH complexes.

4.2. More spectroscopic evidence for $H_2O/CH_3OH/CO_2$

Several other bands in the interstellar ice spectrum toward protostars can be well fitted using an annealed mixture containing H_2O, CH_3OH and CO_2 in equal proportions. Fig. 19 shows the CO stretch of CH_3OH toward GL2136 observed by Skinner et al. (1992) compared to such an annealed mixture.

Although the CO stretch of CH_3OH is embedded in the strong silicate band at $10\,\mu m$ and rather noisy, the laboratory spectrum shows very good similarity in band position and width to the astronomical spectrum. The band can also be reasonably matched with CH_3OH/H_2O mixtures with a ratio larger than

50% (Skinner et al. 1992). The column density ratio is only $\sim$0.1 again indicating that the CH_3OH is part of a separate ice component, not well mixed in with the H_2O ice along the line of sight. Dartois et al. (1999a) observed the ν_3 CH stretching mode and combination modes of CH_3OH using ground based observations toward the massive protostars GL7009S and W33A. The best fit for these CH_3OH bands could be obtained with a combination of pure CH_3OH and an annealed H_2O-CH_3OH-CO_2 mixture as mentioned above.

Additional bands are appearing in the presented study which could also be present in ISO spectra or ground-based data. An absorption feature at $2040\,cm^{-1}$ ($4.9\,\mu m$) is observed toward many lines of sight. It has been matched to the CO stretching mode of OCS (Palumbo et al. 1997). We observed a band at the same position in annealed ($\sim$130 K) $H_2O/CH_3OH/CO_2$ ice mixtures and attribute this to the overtone of CH_3OH. This feature may contribute $\sim$20% to the astronomical band, in good agreement with previous results (Grim et al. 1991, Dartois et al. 1999b).

Observations of RAFGL7009S and NGC 7538 IRS9 reveal an absorption band at $1720\,cm^{-1}$ ($5.8\,\mu m$) which coincides with the CO stretch of H_2CO and HCOOH (d'Hendecourt et al. 1996, Schutte et al. 1996). As shown in Fig. 13 a band at this position appears upon heating of a H_2O:CH_3OH:CO_2 = 1:1:1 mixture to 120 K. In astronomical spectra this feature will however be masked by the strong $6\,\mu m$ bending mode of the bulk H_2O ice.

Fig. 6 shows three bands at $1380\,cm^{-1}$ ($7.24\,\mu m$), $1340\,cm^{-1}$ ($7.46\,\mu m$) and $1276\,cm^{-1}$ ($7.84\,\mu m$) appearing in specific CH_3OH-CO_2 binary mixtures. The $7.24\,\mu m$ and $7.46\,\mu m$ bands roughly coincide with two weak bands that are observed toward several high mass protostars (Schutte et al. 1999). However, the low band strength of the $1380\,cm^{-1}$ feature (Sect. 3.1.2), which is ascribed to a CO_2 inactive mode shows that its contribution to the corresponding weak band observed in W33A is negligible ($< 2\%$).

The $1340\,cm^{-1}$ band of isolated CH_3OH is strongest in mixtures which are rich in CO_2. The ice with the largest apolar component that is still able to fit the observed CO_2 bending mode is H_2O:CH_3OH:CO_2= 70:70:100 (Fig. 10). Using the strength of the $1340\,cm^{-1}$ feature in this ice we find that less than 8% of the corresponding weak band in W33A (at $1349\,cm^{-1}$) can be attributed to the isolated CH_3OH feature.

4.3. Evolution of grain composition

The detection of large amounts of CO_2 throughout the interstellar medium makes it necessary to define the environment where it is present. From astronomical abundance measurements we know that the CO_2/H_2O ratio is rather constant at $\sim$20%. However, the CH_3OH/H_2O ratio varies strongly between different objects. For massive protostars, CH_3OH abundances relative to H_2O vary between 2–30% (Dartois et al. 1999a, Gerakines et al. 1999). Low mass protostars and field stars show low CH_3OH abundances ($CH_3OH/H_2O \leq$2–6%). Abundances derived from ISO data show that a ratio of H_2O:CO_2:CH_3OH = 100:20:10 is a good representative of the conditions near high mass protostars.

As discussed, thermal processing in the laboratory of H_2O dominated mixtures including CH_3OH and CO_2 never leads to the infrared signature which is observed in space. However, a mixture of H_2O:CH_3OH:CO_2 in similar proportions does. Thus, at face value, the laboratory results seem to indicate that near high mass protostars gas condensation on grains leads to ices having very similar abundances of H_2O, CO_2 and CH_3OH. Such a model may find some support in general observations of ices in various regions in dense clouds. The low limits for solid CH_3OH in low mass protostars and field stars indicate that most of the solid CH_3OH near high mass protostars must have been produced locally. In this view the composition of the ice phase in which CH_3OH is embedded simply reflects the chemical circumstances that are characteristic of high mass star forming regions.

In space the accretion of O ensures efficient H_2O formation in the presence of abundant atomic H. CH_3OH may be formed when accreted CO reacts with atomic H (Tielens & Hagen 1982). In models of surface chemistry accreted CO reacts with accreted O to form CO_2. The CO_2 formation occurs likely in environments where the atomic content in the gas phase is important. CO_2 could also be formed by energetic processing. It is yet unclear how surface reactions would form ice layers with H_2O, CO_2 and CH_3OH in similar proportions in the interstellar medium in the vicinity of massive protostars.

Another possibility is that CO_2 and CH_3OH, embedded in a large H_2O matrix, form during heating events different phases, such as clathrate hydrates, boundary phases of pure components and clusters of CO_2-CH_3OH molecules. Although this process cannot be simulated in the laboratory (H_2O dominated mixtures do not allow the formation of the triple peak structure in the CO_2 bend) it might occur during the long timescales in the ISM. Strong Lewis complexes are easily formed between CH_3OH and CO_2 already at 10 K and remain stable below 70 K. Grains might be exposed to heating and thereafter be recooled. The triple-peak structure once formed is stable during recooling. By comparing laboratory data and ISO data we therefore can only prove that in some stage in the evolution of icy grains high temperature events have occured.

The role of UV radiation still has to be further investigated. The general absence of recombination lines in the spectra of protostars and the weakness of the radio-continuum suggests that many sources have not yet reached the stage where UV photoprocessing plays an important role (Gerakines et al. 1999, van der Tak et al. 1999). UV radiation might also be efficiently attenuated in such clouds by dust extinction. In this case the presented laboratory spectra can be used to estimate the evolutionary stage of the protostar by studying the thermal processing of ices (Boogert et al. 1999a).

5. Conclusion

We have presented in this paper a database ($\sim$ 500 spectra) of thermally processed H_2O, CO_2 and CH_3OH ices which can be retrieved from the Leiden observatory database (www.strw.leidenuniv.nl/$\sim$lab/isodb). In comparison with lab-

oratory data ISO has revealed a new ice type, present in the vicinity of massive protostars, which is partly crystallized. From a detailed band profile study we conclude that an ice mixture of H_2O, CO_2 and CH_3OH in similar proportions must be present on grains close to massive protostars. From the laboratory data there is spectroscopic evidence for the presence of segregated "boundary" phases of pure ices, which indicates the presence of clathrates. The CO_2 bending mode as well as H_2O and CH_3OH bands can be efficiently used to estimate the degree of thermal processing in the protostellar enviroment. Laboratory studies showed that annealed ices are more susceptible to UV irradiation than cold amorphous ices. A comparison of observations with laboratory data indicates that we sample different grain populations in the line of sight toward protostars. Therefore only a combination of laboratory mixtures at different temperatures will be fully representative for the overall astronomical infrared spectrum of ices. ISO has set an important example that laboratory data are crucial to reveal the environmental conditions in protostellar regions.

References

Blake D.F., Allamandola J.M., Sandford S.A, Hudgins D., Freund F., 1991, Sci 254, 548

Boogert A.C.A., Schutte W.A., Tielens A.G.G.M., et al., 1996, A&A 315, L377

Boogert A.C.A., Helmich F.P., van Dishoeck E.F., et al., 1998, A&A 336, 352

Boogert A.C.A., Ehrenfreund P., Gerakines P.A., et al., 1999a, A&A in press

Boogert A.C.A., Gerakines P.A., Ehrenfreund P., et al., 1999b, A&A in preparation

Chiar J.E., Gerakines P.A., Whittet D.C.B., et al., 1998, ApJ 498, 716

Dartois E., d'Hendecourt L., Boulanger F., et al., 1998, A&A 331, 651

Dartois E., Schutte W.A., Geballe T.R., et al., 1999a, A&A 342, L32

Dartois E., Demyk K., d'Hendecourt L., Ehrenfreund P., 1999b, A&A, accepted

d'Hendecourt L., Jourdain de Muizon M., Dartois E., et al., 1996, A&A 315, L365

d'Hendecourt L., Joblin C., Jones A., 1999, Solid Interstellar Matter: The ISO Revolution. Springer-Verlag, EDP Sciences

Ehrenfreund P., Boogert A.C.A., Gerakines P.A., et al., 1996a, A&A 315, L341

Ehrenfreund P., Gerakines P.A., Schutte W.A., et al., 1996b, A&A 312, L263

Ehrenfreund P., Boogert A.C.A., Gerakines P.A., et al., 1997, A&A 328, L649

Ehrenfreund P., Dartois E., Demyk K., d'Hendecourt L., 1998, A&A 339, L17

Fleyfel F., Devlin J.P., 1991, J. Phys. Chem. 95, 3811

Fredin L., Nelander B., 1976, Chem. Phys. 15, 473

Gerakines P.A., Schutte W.A., Greenberg J.M., van Dishoeck E.F., 1995, A&A 296, L810

Gerakines P.A., Schutte W.A., Ehrenfreund P., 1996, A&A 312, 289

Gerakines P.A., Whittet D.C.B., Ehrenfreund P., et al., 1999, ApJ 522, 357

de Graauw T., Whittet D.C.B., Gerakines P.A., et al., 1996, A&A 315, L345

Grim R.J.A., Baas F., Geballe T.R., Greenberg J.M., Schutte W.A., 1991, A&A 243, 473

Gürtler J., Henning Th., Koempe C., et al., 1996 A&A 315, L189

Jenniskens P., Blake D.F., 1994, Sci 265, 753

Kerkhof O., Schutte W.A., Ehrenfreund P., 1999, A&A 346, 990

Lacy J.H., Faraji H., Sandford S.A., Allamandola L.J., 1998 ApJ 501, L105

Léger A., Jura M., Omont A., 1985, A&A 144, L147

Mak T.C.W., McMullan R.K., 1964, J. Chem. Phys. 42, L2732

Palumbo M.E., Tielens A.G.G.M., Tokunaga A.T., 1995, ApJ 449, L674

Palumbo M.E., Geballe T.R., Tielens A.G.G.M., et al., 1997, ApJ 479, L839

Palumbo M.E., Baratta G.A., Brucato J.R., et al., 1998, A&A 334, 247

Palumbo M.E., Castorina A.C., Strazulla G., 1999, A&A 342, 551

Sandford S.A., Allamandola L.J., Tielens A.G.G.M., Valero L.J., 1988, ApJ 329, 498

Sandford S.A., Allamandola L.J., 1990, ApJ 355, 357

Sandford S.A., Allamandola L.J., 1993, ApJ 417, 815

Schutte W.A., Greenberg J.M., 1991, A&A 244, L190

Schutte W.A., Tielens A.G.G.M., Whittet D.C.B., et al., 1996, A&A 315, L333

Schutte W.A, Boogert A.C.A, Tielens A.G.G.M., et al., 1999, A&A 343, 966

Serralach A., Meyer R., Guenthard Hs.H., 1974, J. Mol. Spec. 52, 94

Skinner C.J., Tielens A.G.G.M., Barlow M.J., Justtanont K. 1992, ApJ 399, L79

Tielens A.G.G.M., Hagen W., 1982, A&A 114, L245

Tielens A.G.G.M., Tokunaga A.T., Geballe T.R., Baas F., 1991, ApJ 381, L181

van der Tak F.F.S., van Dishoeck E.F., Evans N.J., Blake G.A., 1999, ApJ, to be submitted

van Dishoeck E.F., Helmich F.P., de Graauw T., et al., 1996, A&A 315, L349

van Dishoeck E.F., 1998, Faraday Discussion 109, Chemistry and Physics of Molecules and Grains in Space. The Royal Society of Chemistry, London, 31

Weber P., Greenberg J.M., 1985, Nat 316, L403

Whittet D.C.B., Schutte W.A., Tielens A.G.G.M., et al., 1996, A&A 315, L357

Whittet D.C.B., Gerakines P.A., Tielens A.G.G.M, et al., 1998, ApJ 498, L159

van der Zwet G.P., Allamandola L.J., Baas F., Greenberg J.M., 1989, J. Mol. Structure 195, 213